THE JOURNAL OF PHYSICAL CHEMISTRY C

Article

pubs.acs.org/JPCC

Energetic Stability of Absorbed H in Pd and Pt Nanoparticles in a More Realistic Environment

Sergey M. Kozlov,[†] Hristiyan A. Aleksandrov,[†,‡] and Konstantin M. Neyman*[,†,§]

[†]Departament de Química Física and Institut de Química Teòrica i Computacional (IQTCUB), Universitat de Barcelona, c/Martí i Franquès 1, 08028 Barcelona, Spain

[‡]Faculty of Chemistry and Pharmacy, University of Sofia, 1126 Sofia, Bulgaria

[§]Institucio Catalana de Recerca i Estudis Avançats (ICREA), 08010 Barcelona, Spain

Supporting Information

ABSTRACT: Absorbed hydrogen can dramatically increase hydrogenation activity of Pd nanoparticles and was predicted to do so also for Pt. This calls for investigations of the energetic stability of absorbed H in Pd and Pt using nanoparticle models as realistic as possible, i.e., (i) sufficiently large, (ii) supported, and (iii) precovered by hydrogen. Herein, hydrogen absorption is studied in MgO(100)-supported 1.6 nm large Pd and Pt nanoparticles with surfaces saturated by hydrogen. The effect of surface H on the stability of absorbed H is found to be significant and to exceed the effect of the support. H absorption is calculated to be endothermic in Pt, energy neutral in Pd(111) and bare Pd nanoparticles, and exothermic in H-covered Pd nanoparticles. Hence, we identify the abundance of surface H and the nanostructuring of Pd as prerequisites for facile absorption of hydrogen in Pd and for the concomitantly altered catalytic activity.

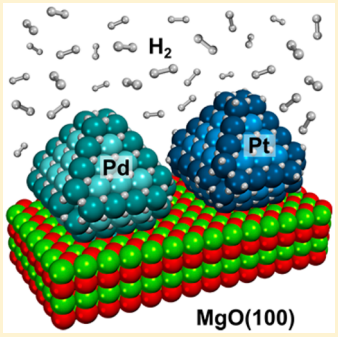

1. INTRODUCTION

Hydrogen, the element with the smallest atoms, is known to be absorbed by some of transition metals under special conditions after their surface is saturated by H.[1] Interplay between adsorbed hydrogen and hydrogen absorbed near surface reveals intriguing consequences for the surface reactivity of late transition metals.[2−7] For instance, density-functional calculations[7] show that the presence of subsurface H in Pd and Pt substantially weakens the binding of adsorbed H species (H^{ads}), making them much more active in hydrogenation reactions. Notably, absorbed H atoms in metal nanoparticles (NPs) affect the binding and the activity of H^{ads} much stronger than in the corresponding (111) single crystals.[7] Also, one may think of a direct recombination of subsurface H with surface adsorbates; for example, this was discussed for Ni(111) and Pd(111) surfaces.[2,7−9]

In view of these findings, the pivotal issue of energetic stability of absorbed H in Pd and Pt nanoparticles should be addressed. Experimentally, Pd nanoparticles provided higher quantities of (released) absorbed H compared to Pd(111) single crystals.[9−11] For instance, Wilde et al. measured for Pd NPs the enthalpy of absorption to be 0.28 ± 0.02 eV per H atom at low concentration of absorbed hydrogen.[12] (Here and in the following positive energy values characterize exothermic processes.) At the same time, the internal energy and the enthalpy of formation of β-phase of Pd hydride in bulk samples were measured to be 0.09 eV lower.[13,14]

There are only few computational studies of H absorption in Pd nanoparticles sufficiently big to be representative of larger experimentally studied species.[15−18] However, these studies either (1) do not explicitly consider stability of H absorbed in Pd nanoparticles compared to gas phase H_2 molecules or to H absorbed in bulk Pd or (2) do not account for a very important fact[7,19,20] that H absorption occurs only in nanoparticles with surface densely covered by H or (3) consider nanoparticles in the unsupported state.

The available literature on H absorption in Pt is less clear. In Pt(111) single crystals absorbed H was found to be present in very small (if any) concentration,[21,22] whereas some studies reported significant H absorption in Pt nanoparticles.[23−25] Computationally H absorption in sufficiently big Pt nanoparticles was addressed without considering surface saturation by adsorbed H atoms.[18]

Herein, we model hydrogen absorption in 1.6 nm large Pd_{127} and Pt_{127} nanoparticles covered by adsorbed H and located on MgO(100) oxide support. In order to disentangle the effect of surface H on the absorption energies from that of metal nanostructuring, the obtained H absorption energies are analyzed in comparison with those calculated on pristine (clean) nanoparticles and extended (111) surfaces. For both metals H^{ads} is found to destabilize hydrogen absorbed in the subsurface region but to stabilize hydrogen absorbed deeper inside. This made H absorption in some sites of Pd nanoparticles covered by H^{ads} by 0.08 eV more exothermic than in Pd bulk. The influence of adsorbed H on H absorption

Received: December 31, 2014
Revised: February 6, 2015
Published: February 6, 2015

DOI: 10.1021/jp513022m
J. Phys. Chem. C 2015, 119, 5180−5186

is found to be notably stronger than the effect induced by clean (100) surface of a defect-free MgO support.

2. COMPUTATIONAL DETAILS

The VASP software package[26] was used to perform electronic structure calculations with the revised Perdew–Burke–Ernzerhof exchange-correlation functional.[27] This functional was shown to be suitable for treatment of H–Pd and H–Pt interactions, despite that it underestimates the strength of interactions of H with Pd by 0.09 eV[18] and overestimates interatomic distances in bulk Pd and Pt[28] even after correction for effects of finite temperature and zero-point vibrations.[29,30] Calculations were carried out using plane waves with the energy cutoff 415 eV in the spin-unpolarized manner. The latter approximation for paramagnetic conducting materials is justified by the rehybridization of electronic states upon H interaction with transition metals discussed by Newns[31] and by explicit computational tests.[32] The interaction between core and valence electrons was described using the PAW technique.[33] During the geometry optimization all H atoms were relaxed, while all Mg and O atoms were kept fixed. The relaxation of MgO(100) support was shown to affect the strength of its binding with Pd NPs by less than 3 meV per metal atom on the interface.[35] All metal atoms composing the NPs were relaxed during the geometry optimization. Out of six layers of the employed p(3 × 3) M(111) slabs only the top four layers were relaxed, while the two bottom layers were fixed on the cut from bulk geometry with the experimental lattice parameter. More computational details can be found in ref 18.

Binding energies of adsorbed and absorbed H were calculated as $E_H = E[H_{N-1}/\text{substrate}] + {}^1/_2E[H_2] - E[H_N/\text{substrate}]$, where $E[H_N/\text{substrate}]$ is the total energy of interacting system of N atoms of H and the substrate, $E[H_{N-1}/\text{substrate}]$ is the energy of this system after removal of the given H atom, and $E[H_2]$ is the energy of the gas phase H_2 molecule. The dissociation energy of the latter was calculated to be 4.57 eV per molecule. No zero-point energy corrections were applied, as justified elsewhere.[18]

The charge density difference was calculated as $\Delta\rho = \rho[H_N/\text{substrate}] - \rho[H_N] - \rho[\text{substrate}]$ with geometries of hydrogen atoms and substrate (MgO supported NPs) fixed on those from optimized H_N/substrate system. The isosurfaces were visualized with VESTA software[34] at the isovalue of ∼20 nm^{-3} (3×10^{-3} $bohr^{-3}$ exactly).

3. EMPLOYED MODELS

The models of supported Pd and Pt NPs employed in this study consist of M_{127} species located on two-layer-thick MgO(100) slabs with p(7 × 7) supercells (Figure 1). There, adjacent NPs are separated by more than 0.7 nm. Increased separation between the NPs or thickness of the MgO slabs were shown not to change the NP–oxide interaction in any significant way.[35]

In this work we considered Pd and Pt nanoparticles with *fcc* lattice structure because the latter is exhibited by bigger NPs commonly dealt with in experiment and application. The shape of employed Pd_{127} and Pt_{127} nanoparticles was optimized in a previous study through extensive screening of feasible NP structures with interatomic potentials (at 0 K) and subsequent evaluation of energetic stability of low-energy species with DFT.[35] The employed shapes are also in line with experimental observations for bigger nanoparticles[36,37] and Wulff–Kaischev

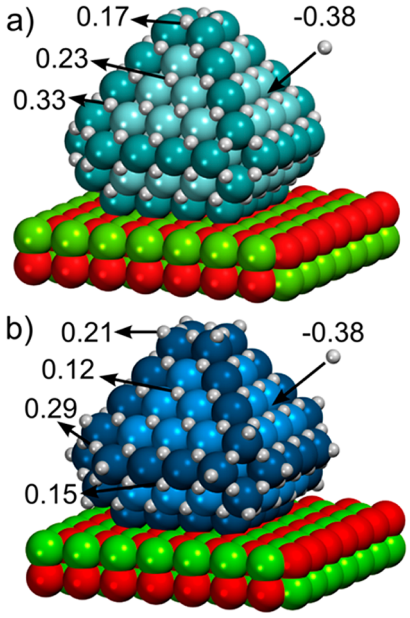

Figure 1. MgO(100)-supported metal nanoparticles saturated by adsorbed H: (a) H_{96}/Pd_{127} and (b) H_{116}/Pt_{127}. Adsorption energies of the present H atoms in various positions (arrows on the left-hand side) and adsorption energy of an additional H atom (arrows on the right-hand side) are given in eV with respect to gas-phase H_2. Pd and Pt atoms on the edges are displayed as turquoise and dark blue spheres; those on the terraces by cyan and light blue spheres, respectively; Mg atoms, green spheres; O atoms, red spheres.

construction. Note that at finite temperatures entropic contributions may favor less regular nanoparticle structures than those presented here.[38−40]

The size of Pd_{127} and Pt_{127} nanoparticles is sufficient to allow *scalability with size* of their adsorptive and absorptive properties.[41] That is, these properties have been shown to vary smoothly and monotonously, when moving from Pd and Pt nanoparticles of >1 nm to bigger species with *fcc* structure.[42,43] Calculations of single H atom on Pd_N and Pt_N (N = 74–140) NPs with gradually varying shape and size in ref 18 revealed minor dependency of H binding energies on any of these two parameters. This finding suggests that the dependency of the effects described herein on nanoparticle shape and size should not be very strong and that the extrapolation of the obtained results onto reasonably similar Pd and Pt NP is appropriate.

The covered by H NP models were generated by successively populating adsorption sites with H atoms until further H adsorption became endothermic (with respect to gas-phase H_2). In such a way it was possible to accommodate 96 H atoms on the supported Pd_{127} NP (Figure 1a). There, H atoms occupied both the 3-fold hollow *fcc* sites on the {111} facets (in line with experimental results for Pd(111) single crystals)[44] and the bridge sites between a pair of metal atoms on the small {100} facets. The supported, surface-saturated with H Pt_{127} NP differs from the respective Pd_{127} NP by the presence of additional 20 H atoms adsorbed on-top of Pt atoms composing the small {100} facets (Figure 1b). Note that there are only 84 metal atoms on NP surface exposed to H, so the resulting coverages of adsorbed H are above 1 ML. Figure 1 displays the corresponding adsorption energies. Further adsorption of H on $H_{96}Pd_{127}$ and $H_{116}Pt_{127}$ is endothermic by 0.38 eV, justifying that surfaces of these nanoparticles are close to be saturated by

DOI: 10.1021/jp513022m
J. Phys. Chem. C 2015, 119, 5180−5186

Table 1. Absorption Energies (in eV per Atom, with Respect to Gas-Phase H_2) of H in (111) Single Crystals and MgO-Supported Nanoparticles of Pd and Pt Depending on the Absorption Site and Presence of Adsorbed H

	Pd(111)		Pd_{127}/MgO(100)		Pt(111)		Pt_{127}/MgO(100)	
site	pristine	H-covered	pristine	H-covered	pristine	H-covered	pristine	H-covered
oss	−0.01	−0.16	0.00	−0.04	−0.43[a]	−0.58	−0.40	−0.45
oss/edge			0.04[a]	−0.26			→*fcc*[b]	−0.54
tss	−0.02	−0.19	−0.01	−0.07	−0.46	−0.56	−0.38[c]	−0.52
tss′	−0.03	−0.10	0.01	−0.01	−0.43	−0.58	−0.26	−0.33
tss/edge[d]			→*hcp*[b]	−0.19			→*bridge*[b]	−0.54
o2ss	−0.12	−0.06	−0.11[a]	0.09	−0.76	−0.69	−0.75	−0.56
t2ss	−0.16	−0.11	−0.13	0.11	−0.73	−0.61	−0.66	−0.55

[a]H in this position was found to be unstable via frequency analysis in ref 18. [b]H escapes from this site during the geometry optimization to the site pointed to by arrow. [c]H migrates from the *tss* site to subsurface site below bridge site composed of two surface and one subsurface Pt atoms. [d]*tss* and *tss′* sites on the edges are structurally identical.

H. Note that no gas phase H_2 molecules were included in calculations.

According to the available experimental data full coverage of Pd and Pt surfaces by H is feasible under certain experimental conditions. For instance, the saturation of Pd(111) with adsorbed H as well as H absorption in Pd can be achieved at 35 °C under 10^{-6} Torr.[45] The case of Pt(111) is more complicated due to notable thermodynamic destabilization of adsorbed H with growing H coverage.[46] The saturation of surface with H was achieved at ultrahigh-vacuum conditions only at temperature of −120 °C. However, during following temperature-programmed desorption experiments a notable fraction (∼1/3) of hydrogen remained on the surface even at 50 °C. In chemical applications at higher H_2 pressures and moderate temperatures one can expect a notably higher degree of saturation of Pt surfaces.

These models were used to study H absorption in interstitial octahedral subsurface *oss* cavities and tetrahedral subsurface *tss* and *tss′* sites between the first and the second surface metal layers. The two types of tetrahedral sites differ by their location below either 3-fold hollow or top surface sites, respectively. For the H absorption between the second and the third surface metal layers we examined tetrahedral *t2ss* and octahedral *o2ss* cavities. Since these sites are not composed of surface metal atoms, we refer to them as bulk sites. We also studied pristine NPs and H-covered and pristine Pd(111) and Pt(111) single crystals.

4. ABSORPTION ENERGIES OF H IN Pd AND Pt

In the absence of surface H absorption energies of hydrogen in Pd(111) single crystals and supported Pd_{127} nanoparticles are calculated to be very close to each other. Namely, H absorption is calculated to be almost energy neutral in subsurface sites and ∼0.1 eV endothermic in deeper "bulk" sites in line with other studies.[47−49] Surface coverage by H^{ads} changes this picture as follows: (1) it *destabilizes* subsurface H by 0.07−0.17 eV on Pd(111) and by 0.02−0.06 eV on Pd NPs; (2) it *stabilizes* bulk hydrogen by ∼0.05 eV on Pd(111) and by 0.20−0.24 eV on Pd NPs. The destabilization of subsurface H is associated with the displacement of the absorbed moieties from the top to the bottom part of the subsurface cavities. For instance, the distance from *oss*-located H in supported Pd_{127} to the nearby surface (subsurface) Pd atoms is around 180 (230) pm when no surface H is present and it changes to 245 (180) pm when the surface is covered by H^{ads}. Note that the destabilizing effect of surface H on absorbed H is smaller on the NPs, whereas the stabilizing effect is larger. It is also worth pointing out that H absorption should be considered feasible in sites with calculated energetic stability around zero, since the employed rPBE exchange-correlation functional somewhat underestimates the strength of H−Pd bonds.[18]

Thus, absorption energy of H in *t2ss* sites of Pd_{127} nanoparticles becomes 0.11 eV upon surface coverage by H^{ads}. At the same time, the formation energy of the hydride Pd_2H is calculated to be only 0.03 eV.[50] Thus, we estimate the combined effect of Pd nanostructuring and surface saturation on the absorption energies of H in Pd to be 0.08 eV, which compares surprisingly well with the stabilization of 0.09 eV derived from measurements.[12−14]

Hence, the effect of nanostructuring on the surface reactivity of Pd is twofold. On the one hand, nanostructuring (in synergy with surface saturation by H^{ads}) promotes H absorption into Pd. On the other hand, nanostructuring has been recently shown to make hydrogenation activity of transition metal catalysts more sensitive to the presence of adsorbed and absorbed H.[7] Both these effects contribute to experimentally observed increase of hydrogenation activity of Pd upon nanostructuring.[4,10]

Note that H atoms are not stable in subsurface sites located at the edges of pristine Pd NPs and escape from them to the surface during geometry optimization calculations (Table 1). Nevertheless, it is possible to stabilize H in these sites by occupying all the *fcc* surface sites on Pd NPs by H atoms. In the latter case, one finds that H in the subsurface sites at the edges is 0.1−0.2 eV less stable than in the terrace subsurface sites. The lower energetic stability can be either intrinsic for H at the edge sites or due to the high number of adsorbed H around these sites. Note that the decreased energetic stability of subsurface H at nanoparticle edges and/or in the presence of surface H may potentially facilitate its direct recombination with various surface adsorbates.

The absorption of H by Pt is significantly energetically unfavorable (Table 1), which agrees with very small concentration of the subsurface H measured in Pt(111).[21] In fact, calculated absorption energies of H in subsurface sites of Pt(111) are in line with the estimated enthalpy of H solution in Pt, −0.48 eV.[1] Similarly to the case of Pd, surface H destabilizes H atoms in subsurface sites of Pt(111) by 0.10−0.15 eV and stabilizes H atoms in the bulk sites by ∼0.1 eV. In turn, on supported Pt nanoparticles subsurface H is destabilized by 0.07−0.14 eV and bulk H is stabilized by 0.11−0.19 eV in the presence of adsorbed H. So the changes of the absorption energies induced by the surface H species are significantly smaller than the intrinsic endothermicity of the H absorption in

DOI: 10.1021/jp513022m
J. Phys. Chem. C 2015, 119, 5180−5186

Pt. Similarly to Pd NPs, we were unable in our calculations to locate H in the subsurface sites at the edges of the pristine Pt NPs. However, the subsurface sites at the edges of Pt NPs covered by adsorbed H are locally stable for H and the absorption energies there are similar to those of the terrace absorption sites in the Pt NPs.

Note that the effect of MgO(100) support on H adsorption and absorption in Pd and Pt nanoparticles was found to be limited to 0.07 eV only.[18] Hence, the surface coverage by H^{ads} is more important for the absorption properties of Pd and Pt nanoparticles than their interaction with MgO(100).

5. EFFECT OF ADSORBED H ON PROPERTIES OF Pd AND Pt

Adsorbed H has a profound effect not only on the absorption properties of the NPs but also on the interatomic distances in the NPs and the electronic structure of the NPs. For instance (see Figure 2), the interatomic distances (average ± standard deviation) change in the supported M_{127} NPs, when their surfaces are covered by H, from 278.8 ± 5.3 to 284.7 ± 3.2 pm for Pd and from 278.3 ± 9.1 to 284.7 ± 6.4 pm for Pt. Thus, H adsorption not only makes average distances in Pd and Pt longer but also decreases their variation within NPs. A qualitatively similar effect of hydrogen on the structure of Al_2O_3-supported Pt nanoparticles was measured in X-ray absorption experiments.[51] However, both the elongation of Pt−Pt contacts and the decrease in standard deviations were measured to be smaller. This could be partially due to the significant effect of Al_2O_3 on the structure of supported Pt clusters, whereas the effect of MgO on geometric structure of supported Pd and Pt nanoparticles was shown to be basically negligible.[35] Interestingly, the increase in the average interatomic distances is not due to the appearance of too long metal−metal contacts but due to the reduced number of short contacts. It can be rationalized by the decreased specific surface energies of the {111} facets upon H adsorption. This reduces the pressure imposed on the NP structures by the facets and consequently leads to the smaller number of short metal−metal distances.

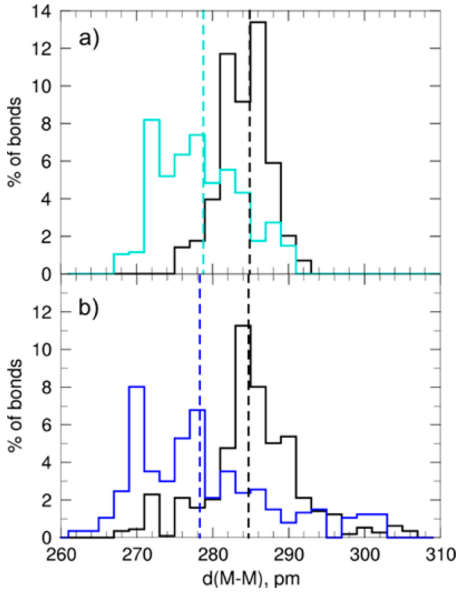

Figure 2. Partition of interatomic distances in pristine (color line) and H-covered (black line) M_{127} NPs supported on MgO: (a) M = Pd; (b) M = Pt. Vertical dashed lines mark average interatomic distances.

The expansion of NPs upon hydrogen adsorption increases the size of interstitial cavities in Pd and Pt and may contribute to higher propensity of the NPs for H absorption. Notably, changes of distances between surface atoms of some bimetallic core−shell NPs by just a few percent have been recently associated with their modified catalytic activity with respect to the monometallic NPs.[52−54] Accordingly, the presently quantified notable structural effects for Pd and Pt NPs imply important modifications in the surface reactivity.

According to the Bader charge analysis,[55] each H atom on the H-covered Pd_{127} NPs accumulates (on average) −0.17 atomic units (au) of charge, which results in the concomitant average charge 0.11 au of Pd atoms. In the H-covered Pt_{127} NPs, the charge on H atoms is around −0.12 au, while Pt atoms are slightly positively charged, by 0.07 au on average. Naturally, one can doubt the numerical accuracy of Bader analysis. However, qualitative predictions of this method seem to be correct for the considered systems, since the electron accumulation on H atoms can be also seen on charge density difference plots (Figure 3). The charge redistribution affects mostly surface metal atoms and may be related to the destabilization of subsurface H in the presence of H^{ads}. The charges on metal atoms are also affected by the electron transfer between the NPs and the MgO(100) support, in which the latter is calculated to donate in total 2.5−3.5 electrons to the deposited NPs.[35] Therefore, the metal−support interactions modify the charge distributions in the metal NPs notably less than the interactions with H atoms can do.

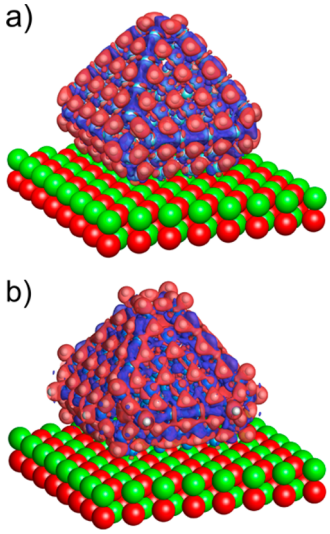

Figure 3. Isosurfaces of charge density difference for adsorption of (a) 96 H atoms on Pd_{127} and (b) 116 H atoms on Pt_{127} on MgO(100) support. Red and blue areas indicate regions of electron accumulation and depletion, respectively. Atoms are displayed like in Figure 1.

There is also a significant effect of the adsorbed H on the electronic structure of the MgO(100)-supported M_{127} NPs (Figure 4), which indicates a dependency of the catalytic properties of Pd and Pt NPs on the amount of H on their surfaces. In the absence of H DOS projected on the metal atoms forming the {111} facets of the NPs are close to the DOS of the metal atoms on the respective (111) surfaces. Upon H adsorption, DOS of the metal atoms shift to lower

DOI: 10.1021/jp513022m
J. Phys. Chem. C 2015, 119, 5180−5186

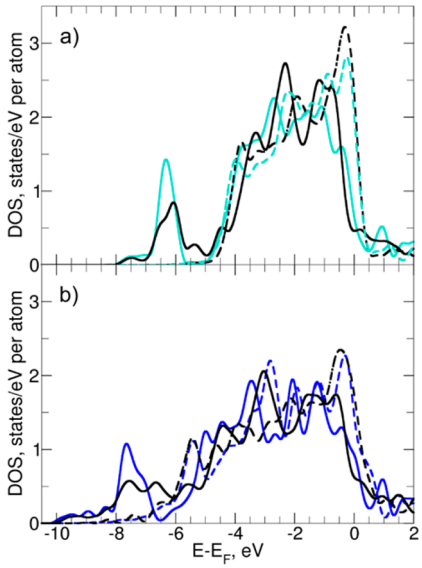

Figure 4. DOS projected on (a) Pd and (b) Pt atoms on {111} terraces of pristine (dashed lines) and covered by H (solid lines) M(111) single crystals (colored lines) and MgO-supported M_{127} NPs (black lines).

energies and the shift is more significant for the NPs than for the single crystals. This means that even if surface reactivity of the NPs is very close to that of the single crystals at low H pressures, the situation may strongly change at higher H pressures and concomitantly higher H surface coverage. In variation, the interaction between supported Pd and Pt NPs and MgO(100) was shown to very slightly modify the electronic structure of the nanoparticles.[35]

6. CONCLUSIONS

To conclude, we found that surface H significantly affects geometric and electronic structure of 1.6 nm large Pd and Pt nanoparticles supported on MgO(100) as well as their absorption properties with respect to H atoms. Surface H is found to destabilize subsurface H atoms and to stabilize H atoms absorbed deeper in the bulk for both nanoparticles and (111) single crystals of Pd and Pt. This made calculated H absorption exothermic in H-covered Pd nanoparticles, in variation with pristine Pd nanoparticles and H-covered and pristine Pd(111) single crystals. In fact, we calculated the difference between H absorption energies in H-covered Pd nanoparticles and infinite Pd bulk to be 0.08 eV, whereas the value of 0.09 eV was estimated from experimental data. Thus, both the nanostructuring and the effect of surface H on nanoparticle properties appear to be required for facile H absorption in Pd. Since absorbed H atoms are known to be essential for certain reactions, this finding helps to explain the effect of nanostructuring on hydrogenation activity of Pd catalysts. In Pt we quantified the absorption of H to be endothermic by at least ~0.45 eV in (111) single crystals and by at least ~0.3 eV in nanoparticles. Thus, our density-functional calculations predict concentration of absorbed H in Pt nanoparticles to be higher than in Pt single crystals but less than the concentration evaluated in experimental studies. Finally, this study demonstrates that the effect of surface coverage and nanostructuring on properties of transition metals is notably stronger than the effect of a rather inert MgO support. This finding is fundamental for the elaboration of realistic, trustworthy, and computationally efficient modeling schemes in a wide range of studies concerning heterogeneous catalysis.

■ ASSOCIATED CONTENT

Supporting Information

Atomic coordinates of selected calculated key structures. This material is available free of charge via the Internet at http://pubs.acs.org.

■ AUTHOR INFORMATION

Corresponding Author

*E-mail konstantin.neyman@icrea.cat; Tel (+34) 93 403 7212; Fax (+34) 93 402 1231 (K.M.N.).

Notes

The authors declare no competing financial interest.

■ ACKNOWLEDGMENTS

Financial support from the Spanish MEDU is gratefully acknowledged (FPU grant AP2009-3379 to S.M.K. and postdoctoral grant SB2010-0172 to H.A.A.). This study was also supported by the European Commission (FP7-NMP.2012.1.1-1 project ChipCAT, ref. no. 310191), the Spanish MINECO (CTQ2012-34969), and the Generalitat de Catalunya (2014SGR97, XRQTC). It is a part of COST Actions CM1104 and MP1103. H.A.A. is grateful to the FP7 programme (project Beyond Everest). The authors thank Red Española de Supercomputación for provided computer resources and technical assistance.

■ REFERENCES

(1) Wilde, M.; Fukutani, K. Hydrogen Detection near Surfaces and Shallow Interfaces with Resonant Nuclear Reaction Analysis. *Surf. Sci. Rep.* **2014**, *69*, 196−295.

(2) Johnson, A. D.; Daley, S. P.; Utz, A. L.; Ceyer, S. T. The Chemistry of Bulk Hydrogen: Reaction of Hydrogen Embedded in Nickel with Adsorbed CH_3. *Science* **1992**, *257*, 223−225.

(3) Brandt, B.; Fischer, J.-H.; Ludwig, W.; Libuda, J.; Zaera, F.; Schauermann, S.; Freund, H.-J. Isomerization and Hydrogenation of cis-2-Butene on Pd Model Catalyst. *J. Phys. Chem. C* **2008**, *112*, 11408−11420.

(4) Doyle, A. M.; Shaikhutdinov, S. K.; Jackson, S. D.; Freund, H.-J. Hydrogenation on Metal Surfaces: Why Are Nanoparticles More Active Than Single Crystals? *Angew. Chem., Int. Ed.* **2003**, *42*, 5240−5243.

(5) Teschner, D.; Borsodi, J.; Wootsch, A.; Révay, Z.; Hävecker, M.; Knop-Gericke, A.; Jackson, S. D.; Schlögl, R. The Roles of Surface Carbon and Hydrogen in Palladium-Catalyzed Alkyne Hydrogenation. *Science* **2008**, *320*, 86−89.

(6) Wilde, M.; Fukutani, K.; Ludwig, W.; Brandt, B.; Fischer, J.-H.; Schauermann, S.; Freund, H.-J. Influence of Carbon Deposition on the Hydrogen Distribution in Pd Nanoparticles and their Reactivity in Olefin Hydrogenation. *Angew. Chem., Int. Ed.* **2008**, *47*, 9289−9293.

(7) Aleksandrov, H. A.; Kozlov, S. M.; Schauermann, S.; Vayssilov, G. N.; Neyman, K. M. How Absorbed Hydrogen Affects Catalytic Activity of Transition Metals. *Angew. Chem., Int. Ed.* **2014**, *53*, 13371−13375.

(8) Henkelman, G.; Arnaldsson, A.; Jónsson, H. Theoretical Calculations of CH_4 and H_2 Associative Desorption from Ni(111): Could Subsurface Hydrogen Play an Important Role? *J. Chem. Phys.* **2006**, *124*, 044706.

(9) Savara, A.; Ludwig, W.; Schauermann, S. Kinetic Evidence for a Non-Langmuir-Hinshelwood Surface Reaction: H/D Exchange over Pd Nanoparticles and Pd(111). *ChemPhysChem* **2013**, *14*, 1686−1695.

DOI: 10.1021/jp513022m
J. Phys. Chem. C 2015, 119, 5180−5186

(10) Doyle, A. M.; Shaikhutdinov, Sh. K.; Freund, H.-J. Alkene Chemistry on the Palladium Surface: Nanoparticles vs Single Crystals. *J. Catal.* **2004**, *223*, 444−453.
(11) Ludwig, W.; Savara, A.; Madix, R. J.; Schauermann, S.; Freund, H.-J. Subsurface Hydrogen Diffusion into Pd Nanoparticles: Role of Low- Coordinated Surface Sites and Facilitation by Carbon. *J. Phys. Chem. C* **2012**, *116*, 3539−3544.
(12) Wilde, M.; Fukutani, K.; Naschitzki, M.; Freund, H.-J. Hydrogen Absorption in Oxide-Supported Palladium Nanocrystals. *Phys. Rev. B* **2008**, *77*, 113412.
(13) Jewell, L. L.; Davis, B. H. Review of Absorption and Adsorption in the Hydrogen-Palladium System. *Appl. Catal., A* **2006**, *310*, 1−15.
(14) Gillespie, L. J.; Ambrose, H. A. The Heat of Absorption of Hydrogen by Palladium Black at 0°. *J. Phys. Chem.* **1931**, *35*, 3105−3110.
(15) Yudanov, I. V.; Neyman, K. M.; Rösch, N. Density Functional Study of Pd Nanoparticles with Subsurface Impurities of Light Element Atoms. *Phys. Chem. Chem. Phys.* **2004**, *6*, 116−123.
(16) Neyman, K. M.; Schauermann, S. Hydrogen Diffusion into Palladium Nanoparticles: Pivotal Promotion by Carbon. *Angew. Chem., Int. Ed.* **2010**, *49*, 4743−4746.
(17) Aleksandrov, H. A.; Viñes, F.; Ludwig, W.; Schauermann, S.; Neyman, K. M. Tuning the Surface Chemistry of Pd by Atomic C and H: A Microscopic Picture. *Chem.—Eur. J.* **2013**, *19*, 1335−1345.
(18) Kozlov, S. M.; Aleksandrov, H. A.; Neyman, K. M. Adsorbed and Subsurface Absorbed Hydrogen Atoms on Bare and MgO(100)-Supported Pd and Pt Nanoparticles. *J. Phys. Chem. C* **2014**, *118*, 15242−15250.
(19) Tao, F.; Salmeron, M. In Situ Studies of Chemistry and Structure of Materials in Reactive Environments. *Science* **2011**, *331*, 171−174.
(20) Lopez, N.; Łodziana, Z.; Illas, F.; Salmeron, M. When Langmuir Is Too Simple: H_2 Dissociation on Pd(111) at High Coverage. *Phys. Rev. Lett.* **2004**, *93*, 146103.
(21) Fukutani, K.; Itoh, A.; Wilde, M.; Matsumoto, M. Zero-Point Vibration of Hydrogen Adsorbed on Si and Pt Surfaces. *Phys. Rev. Lett.* **2002**, *88*, 116101.
(22) Zaera, F. Key Unanswered Questions about the Mechanism of Olefin Hydrogenation Catalysis by Transition-Metal Surfaces: A Surface-Science Perspective. *Phys. Chem. Chem. Phys.* **2013**, *15*, 11988−12003.
(23) Yamauchi, M.; Kobayashi, H.; Kitagawa, H. Hydrogen Storage Mediated by Pd and Pt Nanoparticles. *ChemPhysChem* **2009**, *10*, 2566−2576.
(24) Isobe, Y.; Yamauchi, M.; Ikeda, R.; Kitagawa, H. A Study of Hydrogen Adsorption of Polymer Protected Pt Nanoparticles. *Synth. Met.* **2003**, *135*−*136*, 757−758.
(25) Yamauchi, M.; Kitagawa, H. Hydrogen Absorption in Size-Controlled Pt Nanoparticle. *Chem. Eng. Trans.* **2005**, *8*, 159−163.
(26) Kresse, G.; Furthmuller, J. Efficient Iterative Schemes for ab Initio Total-Energy Calculations Using a Plane-Wave Basis Set. *Phys. Rev. B* **1996**, *54*, 11169−11186.
(27) Hammer, B.; Hansen, L. B.; Nørskov, J. K. Improved Adsorption Energetics within Density-Functional Theory Using Revised Perdew-Burke-Ernzerhof Functionals. *Phys. Rev. B* **1999**, *59*, 7413.
(28) Janthon, P.; Kozlov, S. M.; Viñes, F.; Limtrakul, J.; Illas, F. Establishing the Accuracy of Broadly Used Density Functionals in Describing Bulk Properties of Transition Metals. *J. Chem. Theory Comput.* **2013**, *9*, 1631−1640.
(29) Janthon, P.; Luo, S. A.; Kozlov, S. M.; Viñes, F.; Limtrakul, J.; Truhlar, D. G.; Illas, F. Bulk Properties of Transition Metals: A Challenge for the Design of Universal Density Functionals. *J. Chem. Theory Comput.* **2014**, *10*, 3832−3839.
(30) Lejaeghere, K.; Van Speybroeck, V.; Van Oost, G.; Cottenier, S. Error Estimates for Solid-State Density-Functional Theory Predictions: An Overview by Means of the Ground-State Elemental Crystals. *Crit. Rev. Solid State Mater. Sci.* **2014**, *39*, 1−24.
(31) Newns, D. M. Self-Consistent Model of Hydrogen Chemisorption. *Phys. Rev.* **1969**, *178*, 1123−1135.
(32) Fajín, J. L. C; Cordeiro, M. N. D. S.; Gomes, J. R. B.; Illas, F. On the Need for Spin Polarization in Heterogeneously Catalyzed Reactions on Nonmagnetic Metallic Surfaces. *J. Chem. Theory Comput.* **2012**, *8*, 1737−1743.
(33) Kresse, G.; Joubert, D. From Ultrasoft Pseudopotentials to the Projector Augmented-Wave Method. *Phys. Rev. B* **1999**, *59*, 1758−1775.
(34) Momma, K.; Izumi, F. VESTA 3 for Three-Dimensional Visualization of Crystal, Volumetric and Morphology Data. *J. Appl. Crystallogr.* **2011**, *44*, 1272−1276.
(35) Kozlov, S. M.; Aleksandrov, H. A.; Goniakowski, J.; Neyman, K. M. Effect of MgO(100) Support on Structure and Properties of Pd and Pt Nanoparticles with 49−155 Atoms. *J. Chem. Phys.* **2013**, *139*, 084701.
(36) Olander, J.; Lazzari, R.; Jupille, J.; Mangili, B.; Goniakowski, J. Size- and Temperature-Dependent Epitaxy for a Strong Film-Substrate Mismatch: The Case of Pt/MgO(001). *Phys. Rev. B* **2007**, *76*, 075409.
(37) Revenant, C.; Leroy, F.; Lazzari, R.; Renaud, G.; Henry, C. R. Quantitative Analysis of Grazing Incidence Small-Angle X-Ray Scattering: Pd/MgO(001) Growth. *Phys. Rev. B* **2004**, *69*, 035411.
(38) Lia, Z. H.; Truhlar, D. G. Nanothermodynamics of Metal Nanoparticles. *Chem. Sci.* **2014**, *5*, 2605−2624.
(39) Chang, L. Y.; Barnard, A. S.; Gontard, L. C.; Dunin-Borkowski, R. E. Resolving the Structure of Active Sites on Platinum Catalytic Nanoparticles. *Nano Lett.* **2010**, *10*, 3073−3076.
(40) Stamenkovic, V. R.; Mun, B. S.; Arenz, M.; Mayrhofer, K. J. J.; Lucas, C. A.; Wang, G.; Ross, P. N.; Markovic, N. M. Trends in Electrocatalysis on Extended and Nanoscale Pt-Bimetallic Alloy Surfaces. *Nat. Mater.* **2007**, *6*, 241−247.
(41) Kozlov, S. M.; Neyman, K. M. Catalysis from First Principles: Towards Accounting for the Effects of Nanostructuring. *Top. Catal.* **2013**, *56*, 867−873.
(42) Yudanov, I. V.; Genest, A.; Schauermann, S.; Freund, H.-J.; Rösch, N. Size Dependence of the Adsorption Energy of CO on Metal Nanoparticles: A DFT Search for the Minimum Value. *Nano Lett.* **2012**, *12*, 2134−2139.
(43) Li, L.; Larsen, A. H.; Romero, N. A.; Morozov, V. A.; Glinsvad, C.; Abild-Pedersen, F.; Greeley, J.; Jacobsen, K. W.; Nørskov, J. K. Investigation of Catalytic Finite-Size-Effects of Platinum Metal Clusters. *J. Phys. Chem. Lett.* **2013**, *4*, 222−226.
(44) Mitsui, T.; Rose, M. K.; Fomin, E.; Ogletree, D. F.; Salmeron, M. Hydrogen Adsorption and Diffusion on Pd(111). *Surf. Sci.* **2003**, *540*, 5−11.
(45) Conrad, H.; Ertl, G.; Latta, E. E. Adsorption of Hydrogen on Palladium Single Crystal Surfaces. *Surf. Sci.* **1974**, *41*, 435−446.
(46) Christmann, K.; Ertl, G.; Pignet, T. Adsorption of Hydrogen on a Pt(111) Surface. *Surf. Sci.* **1976**, *54*, 365−392.
(47) Qi, X. Q.; Wei, Z. D.; Li, L.; Ji, M. B.; Li, L. L.; Zhang, Q.; Xia, M. R.; Chen, S. G.; Yang, L. J. DFT Study on Interaction of Hydrogen with Pd(111). *Comput. Theor. Chem.* **2012**, *979*, 96−101.
(48) Greeley, J.; Mavrikakis, M. Surface and Subsurface Hydrogen: Adsorption Properties on Transition Metals and Near-Surface Alloys. *J. Phys. Chem. B* **2005**, *109*, 3460−3471.
(49) Løvvik, O. M.; Olsen, R. A. Adsorption Energies and Ordered Structures of Hydrogen on Pd(111) from Density-Functional Periodic Calculations. *Phys. Rev. B* **1998**, *58*, 10890−10898.
(50) The internal energy of Pd_2H formation becomes 0.07 eV closer to the experimental value of 0.19 eV when zero-point energy corrections are taken into account.
(51) Sanchez, S. I.; Menard, L. D.; Bram, A.; Kang, J. H.; Small, M. W.; Nuzzo, R. G.; Frenkel, A. I. The Emergence of Nonbulk Properties in Supported Metal Clusters: Negative Thermal Expansion and Atomic Disorder in Pt Nanoclusters Supported on γ-Al_2O_3. *J. Am. Chem. Soc.* **2009**, *131*, 7040−7054.
(52) Strasser, P.; Koh, S.; Anniyev, T.; Greeley, J.; More, K.; Yu, C.; Liu, Z.; Kaya, S.; Nordlund, D.; Ogasawara, H.; et al. Lattice-Strain

DOI: 10.1021/jp513022m
J. Phys. Chem. C 2015, 119, 5180−5186

Control of the Activity in Dealloyed Core-Shell Fuel Cell Catalysts. *Nat. Chem.* **2010**, *2*, 454−460.
(53) Shao, M.; Odell, J. H.; Peles, A.; Su, D. The Role of Transition Metals in the Catalytic Activity of Pt Alloys: Quantification of Strain and Ligand Effects. *Chem. Commun.* **2014**, *50*, 2173−2176.
(54) Prabhudev, S.; Bugnet, M.; Bock, C.; Botton, G. A. Strained Lattice with Persistent Atomic Order in Pt_3Fe_2 Intermetallic Core-Shell Nanocatalysts. *ACS Nano* **2013**, *7*, 6103−6110.
(55) Bader, R. F. W. *Atoms in Molecules: A Quantum Theory*; Oxford Science: Oxford, UK, 1990.

DOI: 10.1021/jp513022m
J. Phys. Chem. C 2015, 119, 5180−5186